

Preparation and characterization of mesoporous silica nanoparticles with enlarged pores capped with crosslinked PEI

Lu Sun^{1,2}, Yujie Liu^{1,2}, Zhenzhen Yang^{1,2}, Xianrong Qi^{1,2,3*}

1. Beijing Key Laboratory of Molecular Pharmaceutics and New Drug Delivery System, Peking University Health Science Center, Beijing 100191, China

2. Department of Pharmaceutics, School of Pharmaceutical Sciences, Peking University Health Science Center, Beijing 100191, China

3. State Key Laboratory of Natural and Biomimetic Drugs, School of Pharmaceutical Sciences, Peking University Health Sciences Center, Beijing 100191, China

Abstract: The epidemiological statistics reveals the striking patterns of cancer in women and highlights the need for novel therapeutic strategies. In this work, mesoporous silica nanoparticles (MSNs) as representative of inorganic nanoparticles were prepared for loading siRNA that plays a role of gene silencing to treat breast carcinoma (MCF-7) cells. The critical processes of synthesis were optimized for the nanoparticles with desired quality attributes that have the enlarged pores for elevated loading capacity. After siRNA loading into mesoporous, crosslinked-polyethylenimine was employed as the cap to coat the enlarged MSN pores and protect the cargo from leakage. The elevated quantity of siRNA (35 µg siRNA/mg MSNs) were loaded in the MSNs. The as-synthesized MSNs were further evaluated on MCF-7 cells in vitro and shown negligible cytotoxicity. As expected, the siRNA loaded in the as-synthesized MSNs was readily internalized into MCF-7 cells and displayed 420 times higher intake than that of naked siRNA. The MSNs may be exploited to become an effective siRNA cell delivery strategy and further studied for the anti-tumor efficacy.

Keywords: Mesoporous silica nanoparticle, Preparation, Polyethylenimine, MCF-7 cells

CLC number: R943

Document code: A

Article ID: 1003-1057(2015)11-712-09

1. Introduction

It is noteworthy that GLOBOCAN 2012 has revealed striking patterns of cancer in women and intensively emphasized that the marked increase in breast cancers must be addressed. As the most common cancer and the sixth leading cause of cancer death, breast cancer brings pains on more women of younger generation due to the reproductive, dietary, and hormonal risk factors resulting from the rapid societal, economic changes and a shift towards typical lifestyles of developed countries^[1]. Common treatments of breast cancer including surgery, radiation therapy, systemic treatment with chemotherapy may lead to poorer physical conditions accompanied

by side effects and toxicity to normal cells^[2]. In view of these epidemiological statistics that highlights the increasing incidence of breast cancer in China, novel therapeutic strategies for breast cancer are in urgent need of improvement.

Almost all drugs confront with delivery barriers during the journey from the site of introduction to that of intended target, such as rapid renal filtration and reticuloendothelial system (RES) clearance from the bloodstream, drug internalization of cell, escaping from the acidic environment of endolysosomes, and even crossing the nuclear membrane for cellular targeting^[3-5]. The dilemma conversely motivates the advance of drug delivery system-nanoparticles as representativeness. They offer longer systemic circulation, reduced clearance by the kidneys, increased drug loading capacity due to the large surface area to volume ratio, easy extravasation into tumor tissue from leaky tumor vasculature, and their surfaces modification with various features for a further enhancement of drug delivery^[6-9]. Over the last two decades, a large number of nanoparticle delivery systems

Received: 2015-05-17, Revised: 2015-06-20, Accepted: 2015-07-20.
Foundation items: National Natural Science Foundation of China (Grant No. 81273454 and 81473156), Beijing Nature Science Foundation (Grant No. 7132113), Doctoral Foundation of the Ministry of Education (Grant No. 20130001110055), National Key Basic Research Program (Grant No. 2013CB932501).

*Corresponding author. Tel.: 86-10-82801584,
E-mail: qixr@bjmu.edu.cn

<http://dx.doi.org/10.5246/jcps.2015.11.091>

have been developed for use in cancer therapy and can be classified into two broad categories based upon material composition: organic and inorganic systems. Many liposomes, polymer-drug conjugates, and micellar formulations are front-runners, but other innovative strategies, small inorganic nanoparticles, are entering into the field including metallic nanoparticles made from gold or silver, ceramic nanoparticles made from alumina or silica, quantum dots, and carbon nanoparticles^[6,10,11]. These nanoparticles are not only considered to be generally biocompatible and low toxicity, able to carry diverse drug cargo, and easily modified to increase targeting potential as many other nanoparticle systems, but also possess some characteristics that are not shared with other categories^[6].

Mesoporous silica nanoparticles (MSNs) as a representative inorganic nanoparticles have been comprehensively investigated for various drug delivery application in vitro and in vivo. They have several unique properties that differ from other nanoparticle systems. One is the required extended time of degradation and the structural rigidity which makes them suitable vehicles for long-term controlled-release applications with negligible swelling thus decreasing the probability of burst drug release in systemic circulation^[12,13]. Another is the capacity of incorporating with other characteristics such as magnetism, optical properties that are often unavailable on polymers or metal nanoparticle systems^[14,15]. Mesoporous silica nanoparticles can be divided into three kinds including the traditional MCM-41, SBA-15, and other newly developed types. The most widely investigated type of MSNs is MCM-41, composed of ordered hexagonally arranged cylindrical mesopores^[16]. SBA-15 owns the similar porous framework with MCM-41, but its sizes and pores are bigger and the wall of mesoporous is thicker than that of MCM-41. Other different types of mesostructures including 3D cubic, foam-like, disordered and hollow mesoporous silica have been successfully produced in recent years^[14]. Here, we introduce a MSN of MCM-41 type with larger pores, PEI coating and disulfide bond crosslinking on the surface of the MSN. MCF-7 cells as typical human breast cancer cells were utilized to evaluate the

cytotoxicity and internalization of the MSNs. The MSNs could load more siRNA with negligible cytotoxicity and efficient internalization into MCF-7 cells and is anticipated to be a promising strategy for delivery of siRNA for breast cancer therapies.

2. Materials and methods

2.1. Materials

Tetraethyl orthosilicate (TEOS) and cetyltrimethyl ammonium bromide (CTAB) were obtained from ZKTZ Chemical Technology Co. Ltd. and Biofunction Co. Ltd. (China), respectively. 1,3,5-Trimethylbenzene (TMB) and guanidine hydrochloride were obtained from Sinopharm Chemical Reagent Co. Ltd. (China). Polyethylenimine (PEI, 2 kDa) and dithiobis (succinimidyl propionate) (DSP, Lomant's Reagent) were purchased from Sigma-Aldrich and Thermo Scientific (USA), respectively. FAM-labeled siRNA (FAM-siRNA) (antisense strand, 5'-ACGUGACACGUUCGGAGAATT-3') was purchased from Genepharma (China). RPMI-1640 medium, trypsin, penicillin-streptomycin, and Hoechst 33258 were purchased from Macgene Technology (China).

2.2. Preparation of MSNs

Synthesized silica nanoparticles were prepared as reported previously^[17] with some modifications. CTAB (0.02 mmol) was dissolved in methanol–water (640 g/960 g). With vigorous stirring, NaOH solution (1 M, 45 mL) and TEOS (40 mL) were added to the solution under ambient condition. After being stirred for 8 h, the mixture was aged overnight to obtain white precipitate. Then the synthesized silica nanoparticles were dispersed in ethanol by sonication for 30 min, followed by the addition of 25 mL of 1:1 mixture (v/v) of water and TMB to enlarge the pores in the silica nanoparticles. Two parallel mixtures were placed in a pressure reactor with thick wall, and kept at 140 °C for 48 h or 96 h without stirring.

The resulting white powder was washed with ethanol and water five times each, followed by suspending in 200 mL acidic ethanol solution (100 mL ethanol added

with 1 mL of concentrated hydrochloric acid) to reflux 12 h or 24 h, or calcine in muffle at 300–500 °C. The resulting white powder was filtered out and washed with ethanol followed by drying via nitrogen blowing method or placing in vacuum oven for 12 h.

2.3. Encapsulation of siRNA

To encapsulate siRNA into MSNs, dehydration solution was used as reported previously with some modifications^[18]. The synthesized MSNs (0.3 mg) were dispersed in different ratios of ethanol and guanidine hydrochloride solution followed by adding siRNA, mixed by vortexing for 30 s and continuously shaking at 100 r/min at 25 °C for 1 h. The amount of encapsulated siRNA was calculated from the differences of siRNA concentration in solutions before and after the encapsulation process. siRNA concentration in solution was determined by using Nanodrop 2000 spectrophotometer (Thermo Scientific, USA).

2.4. PEI coating on MSNs to obtain MSN-siRNA/PEI

siRNA-loaded MSNs (MSN-siRNA) were coated with PEI in ethanol by incubation at 25 °C for 20 min and then centrifuged at 5000 r/min for 10 min to remove the free PEI in the supernatant. PEI concentration in ethanol solution was determined using the standard curve plotted by measuring the absorption value at 220 nm with a TU-1900 spectrophotometer. The amount of coated PEI was calculated from the differences of PEI concentration in solutions before and after PEI-coating.

2.5. PEI disulfide bond crosslinking on the surface of MSNs

DSP (0.01 M) in dimethylsulfoxide (DMSO) was added to the obtained aggregates dispersed in ethanol, mixed and incubated together for 30 min to achieve PEI crosslinking by disulfide bond^[19]. Then the obtained MSN-siRNA/CrPEI aggregates were incubated in acidic deionized water under sonication for several minutes and washed with deionized water to obtain the MSN-siRNA/CrPEI nanoparticles.

2.6. Transmission electron microscopy

Transmission electron microscopy (TEM) was carried out on a JEM-2100F transmission electron microscope. Samples were dispersed in ethanol and a drop was placed on the copper grid followed by drying at room temperature for several hours before TEM observation.

2.7. Surface area and porosimetry analysis

Nitrogen adsorption-desorption isotherms were measured at 77 K with 100 mg of MSNs, using an Accelerated Surface Area and Porosimetry System (ASAP 2020). Before the measurements, the samples were degassed at 300 °C for 12 h. Surface area were calculated using the BET multimolecular layer adsorption model and the average pore sizes were calculated from the desorption branch by using the BJH model.

2.8. Thermal gravity analysis

Thermal gravity analysis (TGA) was carried out using a Thermal Gravimetric Analyzer (TGA Q600SDT). About 1 mg of MSNs were measured within the temperature 0–400 °C.

2.9. Zeta potential

The zeta potentials of freshly prepared MSNs were measured using the Malvern Zetasizer Nano ZS (Malvern, UK). Scattered light was detected at a 173 ° backward scattering angle with automatic measurement position and automatic laser attenuation.

2.10. Cell culture

MCF-7 cells were grown in RPMI-1640 medium supplemented with 10% fetal bovine serum, 100 IU/mL penicillin and 100 µg/mL streptomycin. All cells were maintained in a 37 °C humidified incubator in a 5% CO₂ atmosphere.

2.11. Cytotoxicity evaluation

The cytotoxicity of blank carriers of MSN and MSN/CrPEI was determined using the MTT assay. In brief, MCF-7 cells were plated on 96-well plates at the density

of 1×10^5 cells per well in 180 μL complete growth medium and incubated for 24 h. Then the growth medium was replaced with fresh growth medium containing MSN or MSN/CrPEI at various concentrations (ranging from 10 to 100 $\mu\text{g/mL}$). The cells were incubated for another 48 h, followed by the addition of 20 μL MTT solution (5 mg/mL) into each well. After 5 h of incubation at 37 $^\circ\text{C}$ in the cell incubator, the growth medium was removed and 200 μL DMSO was added into each well. Absorbance was measured at a wave length of 570 nm with an iMarkTM microplate absorbance reader (Bio-Rad Laboratories, Hercules, CA, USA).

2.12. Flow cytometry to evaluate cellular uptake

The cellular uptake of the MSNs encapsulated with FAM-siRNA was confirmed by fluorescence detection. MCF-7 cells were seeded in six-well plates at a density of 5×10^5 cells/well in 2 mL of complete 1640 medium for 24 h. The cells were rinsed with PBS and incubated with MSN-siRNA/PEI and MSN-siRNA/CrPEI containing FAM-siRNA (50 nM) in serum-free medium. After incubation for 4 h at 37 $^\circ\text{C}$, the cells were rinsed with cold PBS, trypsinized and washed three times with cold PBS containing heparin (125 U/mL). The samples were centrifuged, resuspended and determined immediately by flow cytometry.

2.13. Confocal fluorescence microscope to evaluate intracellular trafficking

Confocal fluorescence microscope was used to compare the intracellular distribution of the MSNs. MCF-7 cells were seeded on glass-bottom dishes at a density of 2.5×10^5 per well containing complete 1640 medium for 24 h. After three washes with PBS, the MSNs were treated in serum-free medium for 4 h at 37 $^\circ\text{C}$. The final concentration of FAM-siRNA in the culture medium was 50 nM. Subsequently, the cells were rinsed with cold PBS containing heparin (125 U/mL) three times and fixed with 4% formaldehyde for 15 min at room temperature. Following another three rinses with cold PBS, the cell nuclei were stained with Hoechst 33258 (5 mg/mL) for 20 min at 37 $^\circ\text{C}$. Then the cells were imaged using a confocal laser scanning microscope (CLSM, Leica, Heidelberg, Germany). FAM-siRNA and

Hoechst 33258 were excited using 488 nm and 345 nm lasers, respectively.

2.14. Statistical analysis

All data was analyzed using student's *t*-test in statistical evaluation. *P* value < 0.05 was considered to indicate statistically significance (* $P < 0.05$, ** $P < 0.01$, *** $P < 0.005$).

3. Results and discussion

3.1. Preparation of MSNs with enlarged pores at different incubation times with TMB

MCM-41 type of mesoporous silica was synthesized. The MSNs employed here were synthesized based on solution route via CTAB, an alkylammonium salt as liquid crystal templating. In aqueous solution, CTAB self-assembles into micelles or periodic liquid crystal mesophases at concentrations above the critical micelle concentration (CMC). TEOS as the hydrophilic silica precursor is concentrated on the hydrophilic interfaces of micelles via electrostatic and hydrogen bonding interactions, followed by condensing to form an amorphous silica of ordered mesophase^[20].

To improve encapsulation capacity, the pores were enlarged using a hydrophobic swelling agent, TMB, with a suitable size to penetrate into the cores of micelles driven by the hydrophobic force between TMB and surfactant CTAB alkyl chain^[21]. MSNs and TMB were incubated together for different times and subsequently CTAB was removed by refluxing or calcination.

The MSNs incubated with TMB for 48 h showed an average particle diameter around 130 nm and closed porosity (Fig. 1). Whereas, the MSNs incubated with TMB for 96 h showed an average diameter of around 170 nm and clearer porosity as the incubation time extended (Fig. 2). So it is essential for MSNs to be incubated with TMB for enough time to allow most of TMB to penetrate into the micelle rod of CTAB and to expand the hydrophobic core of micelle and even the nanoparticles themselves driven by the hydrophobic forces between TMB and surfactant CTAB alkyl chain, whereas the nanoparticles remained their morphology, monodispersity mesopores^[21].

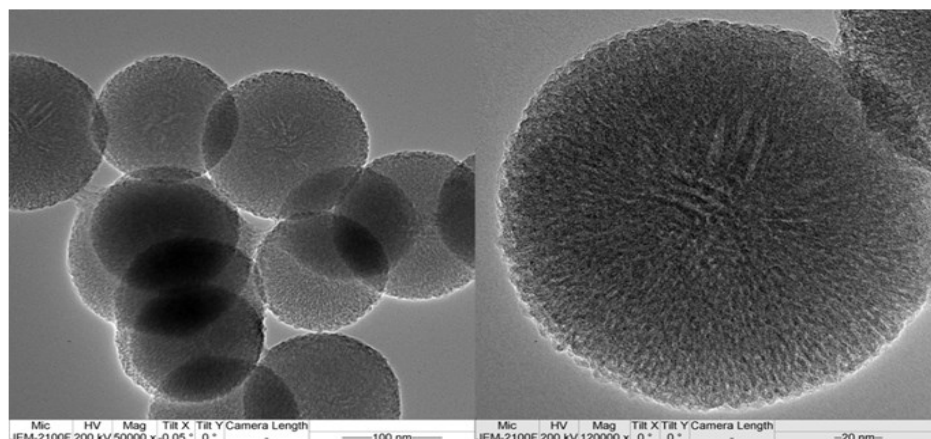


Figure 1. TEM of MSNs obtained by reacting TMB with CTAB for 48 h.

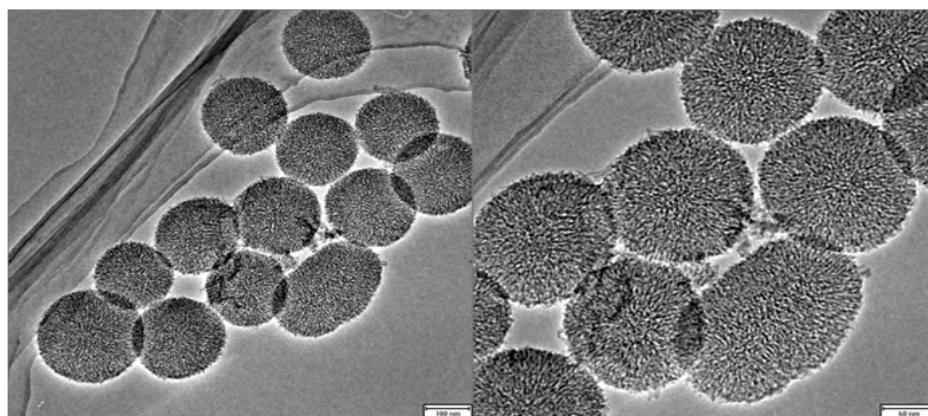


Figure 2. TEM of MSNs obtained by reacting TMB with CTAB for 96 h.

3.2. Removal of surfactant in mesopores

Surfactant remaining in the pores occupies the space, thus not only hindering accurate information of surface area and pores property to be acquired, but also impeding the drug to be adsorbed into the pores. So the removal process is of importance. TGA is a convenient way to estimate whether the surfactant is removed or not. TGA was performed before the surface area and porosimetry analysis and also made sure that the weight would be stable under high temperature.

The reflux time with acidic ethanol had impact on TGA. MSN refluxed for 12 h showed a 1.5% decrease in weight at 230–298 °C, indicating that the residues of CTAB in the pores decomposed to cetene and trimethylamine gas, leading to the loss of weight. After the refluxing for another 12 h, the weight levelled out at 230–298 °C.

Calcining in muffle at 300–500 °C is also a method to remove the residual surfactant, but the critical precondition is slow heating since it is highly possible that the carbonization of residual organic solvent in the MSNs may become brown, thus destroying the surface property of MSNs.

Therefore, refluxing in acid ethanol for adequate time was utilized to remove the surfactant. The method to dry out also influenced the TGA results, thus likely affecting the plotting of nitrogen adsorption-desorption isotherms further. The loss of weight decreased from 7.7% to 2.5% at 0–100 °C after the method was changed from nitrogen blowing to vacuum drying at 100 °C.

3.3. Characteristics of MSNs

MSNs were prepared by keeping the optimized parameters constant. The surface morphology under

TEM revealed the formation of spherical particles. The nitrogen sorption isotherm with a type IV for H_1 hysteresis loop classified by IUPAC indicated the MSNs had the ordered mesopore^[22]. It was shown that BET surface areas were 771.65 m²/g, BJH pore sizes and pore volumes were about 5.7 nm and 1.67 cm³/g, respectively, which are much bigger than those of traditional MCM-41, whose pore size and volume are around 2.7 nm and 1 cm³/g, respectively^[21].

3.4. Encapsulation of siRNA into MSNs

siRNA can be utilized as the drug cargo due to its targeting and efficiency of initiating RNA interference (RNAi), a promising therapeutic modality to treat a variety of diseases. In hydrophilic solution, both siRNA and MSN surfaces are negative and mutually repulsive. However, as the concentration of ions increases, the Debye Length (λ_D) decreases in the chaotropic salt solution^[18], which effectively shields the negative charge and weakens the repulsive electrostatic force between siRNA and MSNs. Chaotropic salt solution containing guanidine hydrochloride (0.667 M) and 66.7% ethanol is adopted^[23]. On one hand, the guanidine cations possess the outstanding ability to catch water molecules, thus offering the shielded intermolecular electrostatic force, dehydration effect, and intermolecular hydrogen bonds. On the other hand, organic solvent induces the dehydrated effect to ensure siRNA to be encapsulated within MSN mesopores^[24]. However, this binding solution has low loading efficiency of merely about 4.6 μ g siRNA per mg MSNs. Considering the facts that the pores of MSNs we used (5.7 nm) were much bigger than those of normal pores (2.7 nm), a larger decline in λ_D is required to facilitate the siRNA absorption into the mesopores. So an elevated concentration of guanidine hydrochloride (0.923 M) and higher percentage of ethanol (76.9%) were used to encapsulate siRNA. The amount of siRNA-loaded by the MSNs could reach 35 μ g siRNA per mg MSNs on average. The result was also in accordance with study to raise percentage of ethanol to increase the amount of siRNA adsorption^[18].

3.5. PEI capping and crosslinking

Low molecular weight PEI (2 kDa) has been utilized to act as the cap and retain cargo due to its positively charge that can be electrostatically attracted to MSNs' surface with intrinsic negative charge via the AS deprotonation of surface silanols^[20]. To prepare PEI-coated MSNs, the siRNA-encapsulated MSNs purified by centrifugation and washing treatments were mixed with PEI in ethanol solution. The standard curve of PEI plotted is shown in Figure 3. The amount of PEI coated on MSNs was 70 μ g/mg. PEI provided the larger number of primary amines as chemical reaction sites for further cross-linking.

The MSNs coated with PEI were subsequently cross-linked with the addition of the appropriate amount of DSP stock solution to generate the desired degree of crosslinking to reduce the toxicity and keep enough amount stably attached on MSNs. The thiol in DSP reacted with primary amines in PEI and constructed amide bonds by only one step reaction (Fig. 4). The molar ratio between DSP and PEI was 2. Based on the calculated amount of PEI, the number of DSP we needed was 8.10×10^{-8} mol/g MSN. A lower zeta potential of MSN-siRNA/CrPEI nanoparticles which was near zero ($+1.9 \pm 1.08$) mV was observed compared with MSN-siRNA/PEI ($+16.9 \pm 0.30$) mV, indicating that the crosslinking of PEI and induced amide bonds were contributed to an acute reduction of protonable primary amines of PEI.

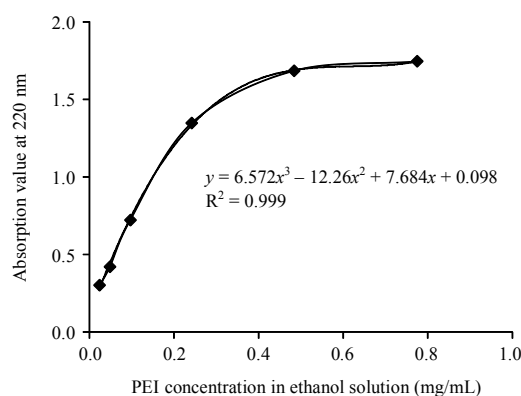


Figure 3. Standard curve of PEI.

3.6. Cytotoxicity on MCF-7 cells

A critical issue for any nanocarrier application is nanoparticle toxicity. The cytotoxicity of as-synthesized nanoparticles and bare MSNs was evaluated on MCF-7 cells using the MTT assay. Figure 5 shows the viability of MCF-7 cells after incubated with MSNs for 48 h. It was found that both bare MSNs and MSN/CrPEI had little toxicity to the cells even though the doses applied were as high as 100 $\mu\text{g}/\text{mL}$, at which the cell viability was no significantly different from that at the lowest dose. The cell viabilities of MSN/CrPEI were almost all higher than 90%, and exhibited little correlation with the dose. It is known that toxicity of PEI is derived from the positively charge that induces the interaction with cells at high dose^[25]. However, the crosslinked short chain PEI showed a lower toxicity than the long chain PEI^[26] due to fewer primary amines and lower positive charge, leading to the lower toxicity of MSN capped with crosslinked PEI.

3.7. Flow cytometry to evaluate cellular uptake of MSNs

MCF-7 cell as typical human breast cancer cell was utilized to evaluate the internalization of the MSNs. Naked FAM-siRNA and FAM-siRNA-loaded MSNs (MSN-siRNA/CrPEI and MSN-siRNA/PEI) containing 50 nM FAM-siRNA, together with MCF-7 cells were incubated for 4 h at 37 °C. The result of flow cytometry is shown in Figure 6. Naked siRNA showed low fluorescence intensity, indicating little translocation of siRNA into the cells. This inefficiency of internalization was consistent with the nature that was poor membrane permeability and hydrophilic nature of naked siRNA^[27]. As expected, both MSN-siRNA/CrPEI and MSN-siRNA/PEI had notably higher intake than the control and about 420 and 250 times higher intake than naked siRNA, respectively. Additionally, approximate 1.8 times uptake of FAM-siRNA was presented by MSN-siRNA/CrPEI relative to MSN-siRNA/PEI that was only capped with PEI, suggesting a significant more translocation of siRNA into the cells. It is likely that short chain and uncrosslinked PEI which has lower electric charge might be less stable and easier to fall off

from MSN surface than the crosslinked PEI, resulting in more leakage of siRNA when electropositive PEI is contacting with electronegative cell membranes. But this explanation is an assumption that needs further verification.

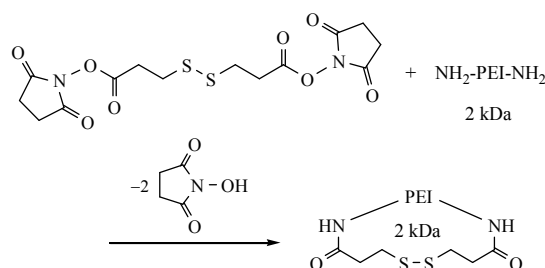


Figure 4. Crosslinking reaction for primary amines of PEI and dithiobis (succinimidyl propionate) (DSP). A reduction of protonable primary amines of the polymer results in the formation of amide bonds.

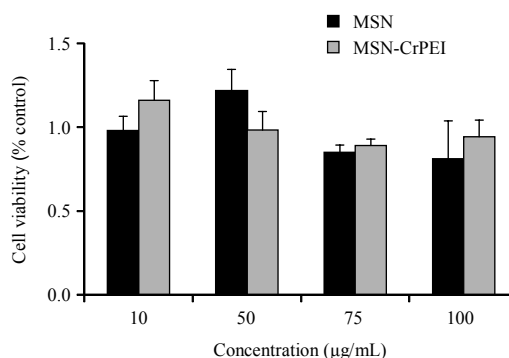


Figure 5. The survival rate of MCF-7 cells after cultured with bare MSN and MSN/CrPEI at the same MSNs dose for 48 h, respectively. Data are presented as the mean \pm SD ($n = 4$).

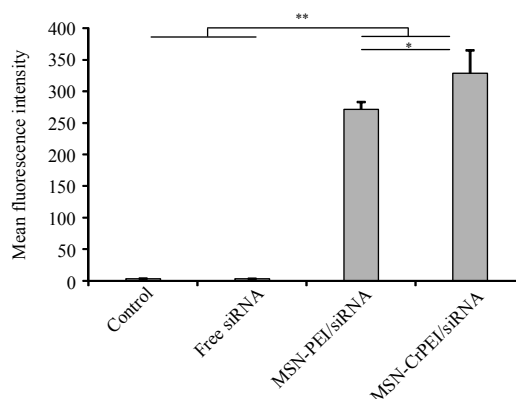


Figure 6. Cellular uptake of FAM-siRNA delivered by MSNs. Fluorescence intensity of MCF-7 cells incubated with naked siRNA, MSN-siRNA/CrPEI, MSN-siRNA/PEI at 37 °C for 4 h was measured using flow cytometry. Cells treated with serum-free media were used as control. The data are expressed as the mean \pm SD ($n = 3$). ** $P < 0.001$, * $P < 0.05$.

3.8. Confocal fluorescence microscopy to evaluate intracellular trafficking of MSNs

Intracellular trafficking of MSNs in MCF-7 cells was evaluated by the confocal fluorescence microscopy (Fig. 7), and the results were consistent with those obtained with flow cytometry. The green fluorescent dots in the cytoplasm suggested that the nanoparticles had been internalized in the cells.

The cells observed under laser scanning confocal microscope were three-dimensional. Where as fluorescence emitted from the cell surface might be masked by the fluorescence emitted from inside the cell when the scanning position was improper, leading to false positive results. In order to eliminate this, cross-sections of the three-dimensional cells were scanned at 1 μm thickness using the unique technology of confocal microscope (Fig. 8). In the MCF-7 cells, the scanning of cross-section at micron level revealed that there was green fluorescence on all layers indicating that the fluorescence of FAM-siRNA was from inside rather than from outside the cells. Confocal scanning technology ruled out the false positive, and proved that the MSN-siRNA/CrPEI could be effectively internalized into the cells.

4. Conclusion

A siRNA delivery system (MSN-siRNA/CrPEI) was prepared through synthesis of MSNs, encapsulation of siRNA into the mesopores of MSNs (MSN-siRNA), PEI-capped MSN-siRNA (MSN-siRNA/PEI), and cross-linking PEI via disulfide bond (MSN-siRNA/CrPEI). Synthesis with optimized critical processes rendered the MSNs with desired quality attributes. After coating with PEI and crosslinking with PEI, the delivery system (MSN-siRNA/CrPEI) was further evaluated on MCF-7 cells, and shown to have negligible cytotoxicity and the ability of efficient internalization into cells. Overall, MSN-siRNA/CrPEI is believed to be an effective strategy for siRNA delivery in future.

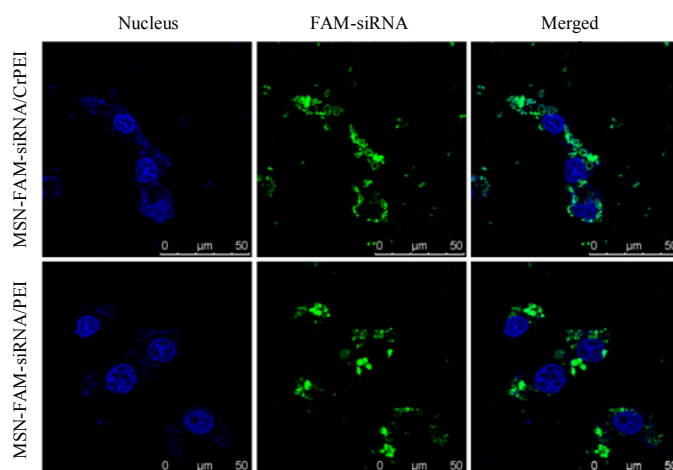


Figure 7. Intracellular trafficking of FAM-siRNA (50 nM) delivered by MSN-siRNA/CrPEI and MSN-siRNA/PEI incubated with MCF-7 cells for 4 h.

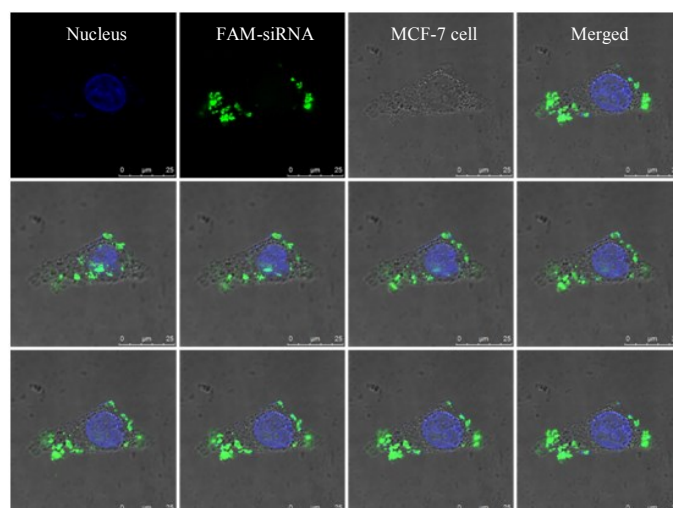


Figure 8. The serial section images of the intracellular distribution after incubation with MSN-siRNA/CrPEI for 4 h. The concentration of FAM-siRNA was 50 nM.

Acknowledgements

This work was supported by National Natural Science Foundation of China (Grant No. 81273454 and 81473156), Beijing Nature Science Foundation (Grant No. 7132113), Doctoral Foundation of the Ministry of Education (Grant No. 20130001110055), National Key Basic Research Program (Grant No. 2013CB932501).

References

- [1] Fan, L.; Strasser-Weippl, K.; Li, J.J.; St Louis, J.; Finkelstein, D.M.; Yu, K.D.; Chen, W.Q.; Shao, Z.M.; Goss, P.E. *Lancet Oncol.* **2014**, *15*, 279–289.

- [2] DeSantis, C.E.; Lin, C.C.; Mariotto, A.B.; Siegel, R.L.; Stein, K.D.; Kramer, J.L.; Alteri, R.; Robbins, A.S.; Jemal, A. *CA Cancer J. Clin.* **2014**, *64*, 252–271.
- [3] Hubbell, J.A.; Chilkoti, A. *Science*. **2012**, *337*, 303–305.
- [4] Dong, D.W.; Xiang, B.; Gao, W.; Yang, Z.Z.; Li, J.Q.; Qi, X.R. *Biomaterials*. **2013**, *34*, 4849–4859.
- [5] Yang, Z.Z.; Li, J.Q.; Wang, Z.Z.; Dong, D.W.; Qi, X.R. *Biomaterials*. **2014**, *35*, 5226–5239.
- [6] Mishra, D.; Hubenak, J.R.; Mathur, A.B. *J. Biomed. Mater. Res. A*. **2013**, *101*, 3646–3660.
- [7] Gao, W.; Xiang, B.; Meng, T.T.; Liu, F.; Qi, X.R. *Biomaterials*. **2013**, *34*, 4137–4149.
- [8] Wang, A.; Tong, S.; Hu, X.; Qi, X.R. *J. Chin. Pharm. Sci.* **2015**, *24*, 419–426.
- [9] Li, J.; Yang, Z.; Meng, T.; Qi, X.R. *J. Chin. Pharm. Sci.* **2014**, *23*, 667–673.
- [10] Heneweer, C.; Gendy, S.E.M.; Peñate-Medina, O. *Ther. Deliv.* **2012**, *3*, 645–656.
- [11] Alexis, F.; Pridgen, E.; Langer, R.; Farokhzad, O. *Drug Delivery*. Springer Berlin Heidelberg. **2010**, *197*, 55–86.
- [12] Sekhon, B.S.; Kamboj, S.R. *Nanomed. Nanotechnol.* **2010**, *6*, 612–618.
- [13] Saravanakumar, G.; Jo, D.G.; Park, J.H. *Curr. Med. Chem.* **2012**, *19*, 3212–3229.
- [14] Yang, L.; Sheldon, B.W.; Webster, T.J. *Am. Ceram. Soc. Bull.* **2010**, *89*, 24–31.
- [15] Slowing, I.I.; Vivero-Escoto, J.L.; Wu, C.W.; Lin, V.S.Y. *Adv. Drug Deliv. Rev.* **2008**, *60*, 1278–1288.
- [16] Tarn, D.; Ashley, C.E.; Xue, M.; Carnes, E.C.; Zink, J.I.; Brinker, C.J. *Acc. Chem. Res.* **2013**, *46*, 792–801.
- [17] Kim, M.H.; Na, H.K.; Kim, Y.K.; Ryoo, S.R.; Cho, H.S.; Lee, K.E.; Jeon, H.; Ryoo, R.; Min, D.H. *ACS Nano*. **2011**, *5*, 3568–3576.
- [18] Li, X.; Xie, Q.R.; Zhang, J.; Xia, W.; Gu, H. *Biomaterials*. **2011**, *32*, 9546–9556.
- [19] Neu, M.; Germershaus, O.; Mao, S.; Voigt, K.H.; Behe, M.; Kissel, T. *J. Control. Release*. **2007**, *118*, 370–380.
- [20] Tarn, D.; Ashley, C.E.; Xue, M.; Carnes, E.C.; Zink, J.I.; Brinker, C.J. *Acc. Chem. Res.* **2013**, *46*, 792–801.
- [21] Mizutani, M.; Yamada, Y.; Nakamura, T.; Yano, K. *Chem. Mater.* **2008**, *20*, 4777–4782.
- [22] Li, X.; Zhang, J.; Gu, H. *Langmuir*. **2011**, *27*, 6099–6106.
- [23] Li, X.; Chen, Y.; Wang, M.; Ma, Y.; Xia, W.; Gu, H. *Biomaterials*. **2013**, *34*, 1391–1401.
- [24] Piotr, C.; Nicoletta, S. *Nat. Protoc.* **2006**, *1*, 581–585.
- [25] Hoon-Jeong, J.; Christensen, L.V.; Yockman, J.W.; Zhong, Z.; Engbersen, J.F.; Kim, W.J.; Feijen, J.; Kim, S.W. *Biomaterials*. **2007**, *28*, 1912–1917.
- [26] Deng, R.; Yue, Y.; Jin, F.; Chen, Y.; Kung, H.F.; Lin, M.C.M.; Wu, C. *J. Control. Release*. **2009**, *140*, 40–46.
- [27] Aagaard, L.; Rossi, J.J. *Adv. Drug Deliv. Rev.* **2007**, *59*, 75–86.

包被交联PEI的拓孔介孔硅的制备与表征

孙璐^{1,2}, 刘瑜洁^{1,2}, 仰湏臻^{1,2}, 齐宪荣^{1,2,3*}

1. 北京大学医学部 分子药剂学与新释药系统北京市重点实验室, 北京 100191
2. 北京大学医学部 药学院 药剂学系, 北京 100191
3. 北京大学医学部 天然药物及仿生药物国家重点实验室, 北京 100191

摘要: 流行病学统计数据揭示了女性群体患癌频率高发的现状, 以及对于新的治疗策略的迫切需要。本研究合成了一种代表性的无机纳米材料的纳米粒——介孔二氧化硅纳米粒递送小干扰RNA, 并通过siRNA发挥基因沉默作用治疗乳腺癌。本研究对介孔二氧化硅纳米粒的合成的关键工序进行优化, 使得所制备的纳米粒具有所需的性质, 即通过拓孔来高载药量。装载siRNA进入介孔内后, 用交联聚乙烯亚胺包被在介孔硅的表面, 作为的孔的“保护帽”, 保护孔内的药物不被泄露。siRNA的载药量可达35 μg siRNA/mg MSNs。随后, MSN-siRNA/CrPEI作为药物递送系统在MCF-7细胞上进行体外水平的评价, 结果表明该载体具有微弱的毒性和易于摄取的特性, 摄取量比裸siRNA提高了420倍。MSN-siRNA/CrPEI可以成为siRNA的有效的递送策略, 可进一步进行抗肿瘤药效学的研究。

关键词: 介孔二氧化硅纳米粒; 制备; 聚乙烯亚胺; MCF-7细胞